MODEL-INDEPENDENT ELECTRON SPIN RESONANCE FOR MEASURING ORDER OF IMMOBILE COMPONENTS IN A BIOLOGICAL ASSEMBLY

THOMAS P. BURGHARDT* AND NANCY L. THOMPSON‡
*841 HSW, Cardiovascular Research Institute, University of California at San Francisco, San Francisco, California 94143; ‡Department of Chemistry, Stanford University, Stanford, California 94305

ABSTRACT A model-independent description of the angular orientation distribution of elements in an ordered biological assembly is applied to the electron spin resonance (ESR) technique. As in a previous model-independent treatment of fluorescence polarization (Burghardt, T. P., 1984, *Biopolymers*, 23:2383–2406) the elemental order is described by an angular distribution of molecular frames with one frame fixed in each element of the assembly. The distribution is expanded in a complete orthonormal set of functions. The coefficients of the series expansion (the order parameters) describe the orientation distribution of the elements in the assembly without reference to a model and can be obtained from the observed spectrum. The method establishes the limitations of ESR in detecting order in the assembly by determining which distribution coefficients the technique can detect. A method of determining the order parameters from an ESR spectra, using a set of ESR basis spectra, is developed. We also describe a treatment that incorporates the actual line shape measured from randomly oriented, immobile elements. In this treatment, no model-dependent assumptions about the line shape are required. We have applied the model-independent analysis to ESR spectra from spin-labeled myosin cross-bridges in muscle fibers. The results contain detailed information on the spin-probe angular distribution and differ in interesting ways from previous model-dependent interpretations of the spectra.

INTRODUCTION

The model-independent description of order in biological assemblies has been developed for use with polarized fluorescence techniques. In these techniques extrinsic fluorescent probes are specifically attached to elements of the biological assembly, e.g., the subfragment-1 (S-1) moiety of a myosin cross-bridge in a muscle fiber, and the orientations of the absorption and/or emission dipole vectors report the angular arrangement of the elements to which the group is attached (Burghardt, 1984; Morales, 1984; Burghardt et al., 1983; Wilson and Mendelson, 1983; Borejdo et al., 1982; Thompson et al., 1984). In electron spin resonance (ESR) techniques, extrinsic spin probes that are also specifically attached to elements of the assembly report the angular arrangement of the elements (Thomas and Cooke, 1980; Cooke et al., 1982; Libertini et al., 1974; Hentschel et al., 1978; Friesner et al., 1979). Here we extend the model-independent description of order in a biological assembly for use with ESR spectra. It is assumed throughout this paper that all motions contributing to the relaxation of the spin probe have characteristic times >300 ns. We demonstrate the usefulness of the model-independent method by fitting spectra from spin-labeled myosin cross-bridges in muscle fibers. The model-independent analysis yields new information about the order of the labeled cross-bridges in the muscle fiber.

The basis of the model-independent method is the description of the elemental order of the biological assembly as an angular distribution of elemental or molecular coordinate frames, with one frame fixed in each element. This distribution is expanded in a complete set of angular functions, and the expansion coefficients, or order parameters (Polnaszek and Freed, 1975), of the distribution are related to the observable ESR spectrum. The distribution coefficients uniquely describe the angular distribution of elements. As in the case of model-independent fluorescence polarization analysis, model-independent ESR analysis establishes the theoretical limitations of the ESR technique for determining elemental order in the biological assembly.

THE MODEL-INDEPENDENT DESCRIPTION OF ESR

We define the analytic function $N(\Omega)$ as the angular distribution of a coordinate frame that is fixed to an element of the biological assembly, e.g., the hydrodynamic

Dr. N. Thompson's present address is the Department of Chemistry, University of North Carolina at Chapel Hill, Chapel Hill, NC 27514.

principal axis frame of S-1 of a myosin cross-bridge. Euler angles α, β, and γ (Davydov, 1966), represented by Ω, determine the orientation of this frame relative to the laboratory frame. In ESR experiments a spin probe is specifically attached to each element so that its principal magnetic axis is, in general, another Euler rotation, denoted by Ω_0, from a given molecular frame at Ω. Angle Ω_0 is constant for all spin probes in a given assembly. The spin-labeled system is placed in a static magnetic field H and is illuminated with circularly polarized microwave radiation. The absorption probability of the microwave energy by a single immobile spin probe, $G(H, \Omega)$, is a function of the strength of the static magnetic field H and its direction relative to the orientation of the element to which the probe is attached. The observed absorption for a macroscopic sample, made up of many spin probes attached to elements with an angular distribution $N(\Omega)$, is called $F(H)$ and is given by

$$F(H) = \int_{C_0} d\Omega\, G^*(H, \Omega) N(\Omega). \tag{1}$$

The domain of integration C_0 is all angular space and the asterisk denotes a complex conjugate. Functions $N(\Omega)$ and $G(H, \Omega)$ are expanded in the Wigner rotation matrix elements $D^{\ell}_{m,n}(\Omega)$ that form a complete set in angular space (Davydov, 1966). We find:

$$N(\Omega) = \sum_{\ell=0}^{\infty} \sum_{m,n=-\ell}^{\ell} a^{\ell}_{m,n} \left(\frac{2\ell+1}{8\pi^2}\right)^{1/2} D^{\ell}_{m,n}(\Omega) \tag{2a}$$

$$G(H, \Omega) = \sum_{\ell=0}^{\infty} \sum_{m,n=-\ell}^{\ell} g^{\ell}_{m,n}(H) \left(\frac{2\ell+1}{8\pi^2}\right)^{1/2} D^{\ell}_{m,n}(\Omega). \tag{2b}$$

Orthogonality of the $D^{\ell}_{m,n}(\Omega)$'s (Davydov, 1966) implies:

$$\int_{C_0} d\Omega\, D^{*\ell'}_{m',n'}(\Omega)\, D^{\ell}_{m,n}(\Omega) = \left(\frac{8\pi^2}{2\ell+1}\right) \delta_{\ell',\ell}\, \delta_{m',m}\, \delta_{n',n}, \tag{3}$$

where $\delta_{i,j}$ is a Kronicker delta. Substituting Eqs. 2a and 2b into Eq. 1 and using Eq. 3 we find

$$F(H) = \sum_{\ell=0}^{\infty} \sum_{m,n=-\ell}^{\ell} a^{\ell}_{m,n}\, g^{*\ell}_{m,n}(H). \tag{4}$$

Eq. 3 also implies from Eq. 2 that

$$a^{\ell}_{m,n} = \left(\frac{2\ell+1}{8\pi^2}\right)^{1/2} \int_{C_0} d\Omega\, D^{*\ell}_{m,n}(\Omega)\, N(\Omega) \tag{5a}$$

$$g^{\ell}_{m,n}(H) = \left(\frac{2\ell+1}{8\pi^2}\right)^{1/2} \int_{C_0} d\Omega\, D^{*\ell}_{m,n}(\Omega)\, G(H, \Omega). \tag{5b}$$

The coefficients $g^{\ell}_{m,n}(H)$ are calculated using Eq. 5b from the line shape $G(H, \Omega)$. Moments $a^{\ell}_{m,n}$, also called order parameters, describe the orientation distribution of elements in the biological assembly, and are what we wish to measure from observation of $F(H)$. We show in a later section that, given $g^{\ell}_{m,n}(H)$, we can measure $a^{\ell}_{m,n}$ from the spectrum $F(H)$.

Form of the Line Shape $G(H, \Omega)$

Simple Treatment. The explicit form of $G(H, \Omega)$ for a nitroxide probe is generally assumed to be a Lorentzian (see e.g., Hudson and Luckhurst, 1968, or Berliner, 1976) such that

$$G(H, \Omega) = \sum_{I} \frac{\epsilon}{\epsilon^2 + [H - H^I_0(\Omega)]^2}, \tag{6}$$

where ϵ is the characteristic width of the Lorentzian, H is the applied static magnetic field, and $H^I_0(\Omega)$ are the resonance static magnetic field values derived from the spin Hamiltonian. For a spin Hamiltonian appropriate for nitroxide spin probes, $H^I_0(\Omega)$ have been shown to be (McCalley et al., 1972; Berliner, 1976)

$$H^I_0(\Omega) = \frac{2\pi\nu - m_I |\gamma_e| |\underline{T} \cdot \mathbf{K}_{lab}|}{|\gamma_e| |\underline{g} \cdot \mathbf{K}_{lab}|}, \tag{7}$$

where ν is the frequency of the microwave radiation, $m_I = -1, 0, 1$ is the nuclear spin projection quantum number, $\gamma_e = -17.6 \times 10^6 s^{-1} G^{-1}$ is the electron gyromagnetic ratio, $\underline{T}$ is the tensor coupling nuclear spin with electron spin, $\mathbf{K}_{lab}$ is a unit vector in the direction of the static magnetic field, and $\underline{g}$ is the tensor coupling electron spin with the applied static magnetic field. The line width ϵ is $1/(|\gamma_e|\tau_2)$, where τ_2 is the spin-spin relaxation time (McCalley et al., 1972).

Usually in ESR experiments the first derivative of the absorption spectrum is detected rather than the absorption spectrum. In this case $G(H, \Omega)$ is replaced by

$$\frac{d}{dH} G(H, \Omega) = \sum_{I} \frac{2\epsilon\,[H^I_0(\Omega) - H]}{\{\epsilon^2 + [H - H^I_0(\Omega)]^2\}^2} \tag{8}$$

in the following equations.

With the expression for $G(H, \Omega)$ given by Eqs. 6 and 7 we can calculate the coefficients $g^{\ell}_{m,n}(H)$ defined in Eq. 5b. We begin by expressing the unit vector $\mathbf{K}_{lab}$, that is parallel to the static magnetic field in the lab frame, in terms of the principal magnetic frame of the spin probe. We do this by applying two successive coordinate rotations: first, a rotation through Euler angles Ω from the lab frame to the molecular frame of the labeled element; second, a rotation through Euler angles Ω_0, from this molecular frame to the principal magnetic frame of the spin probe. (The principle magnetic frame is the frame in which $\underline{g}$ and $\underline{T}$ are diagonal.) The angles Ω vary with the orientation of the element, and the angles Ω_0 are constant because the probe is bound identically to each element.

The unit vector $\mathbf{K}_{lab}$ in the principal magnetic frame is given by

$$\mathbf{K}(\Omega) = M(\Omega_0)\, M(\Omega)\, \mathbf{K}_{lab}, \tag{9}$$

where M is the Euler rotation matrix (Goldstein, 1980).

In the principal magnetic frame the tensors $\underline{g}$ and $\underline{T}$ are diagonal and of the form

$$\underline{g} = \begin{pmatrix} g_x & 0 & 0 \\ 0 & g_y & 0 \\ 0 & 0 & g_z \end{pmatrix} \qquad \underline{T} = \begin{pmatrix} T_x & 0 & 0 \\ 0 & T_y & 0 \\ 0 & 0 & T_z \end{pmatrix}. \tag{10}$$

Substituting $\mathbf{K}(\Omega)$, $\underline{g}$, and $\underline{T}$ into Eq. 7 and using Eq. 7 in Eqs. 6 and 5b enables us to numerically calculate the basis spectra $g^{\ell}_{m,n}(H)$. In general, some of the $g^{\ell}_{m,n}$'s are zero because of symmetry properties of $G(H, \Omega)$ and $D^{\ell}_{m,n}(\Omega)$ as functions of the Euler angles. The zeroes correspond to distribution coefficients ESR cannot detect. These properties of the $g^{\ell}_{m,n}$'s are discussed in a later section.

Generalized Treatment. The reliability of the assumption that $G(H, \Omega)$ is a Lorentzian can be tested experimentally by analyzing a spectrum from immobilized, randomly oriented spin probes (Goldman et al., 1972). This spectrum should be measured from spin probes that are in the same environment as when they are employed to measure the angular distribution of the ordered assembly, so that the appropriate experimental values of the coupling tensors $\underline{g}$ and $\underline{T}$ can be determined.

In general, although the Lorentzian line shape is a good approximation to the real line shape, a better estimation of the real line shape can be made with an orthogonal polynomial expansion such that

$$G(H, \Omega) = \frac{2}{3\epsilon} \sum_{I} \sum_{n=0}^{\infty} h_n P_n[y_I(H, \Omega)], \tag{11}$$

where P_n is the Legendre polynomial, the h_n are constants, and

$$y_I(H, \Omega) \equiv \frac{H - H^I_0(\Omega)}{\{\epsilon^2 + [H - H^I_0(\Omega)]^2\}^{1/2}}. \tag{12}$$

Functions y_I have the range $-1 \le y_I \le 1$ when $0 \le H \le \infty$. The series expansion in Eq. 11 is the Lorentzian shown in Eq. 6 when $h_0 = -h_2 = 1$ and all other h_n's = 0.

The line shape of Eq. 11 can in principle fit any line shape to any accuracy. Only a few terms in the series are necessary when the real line shape is close to Lorentzian. A similar series expansion in Hermite polynomials (Arfken, 1970) can be constructed for real line shapes that to lowest order approximation most resemble a Gaussian form (Goldman et al., 1972).

The line shape parameters h_n are calculated directly from the random, immobile ESR spectrum by a method analogous to the method employed in measuring order parameters. This procedure is described in the next section. The generalized line shape is implemented in the calculation of $g^{\ell}_{m,n}(H)$ by replacing Eq. 6 with Eq. 11 in the Simple Treatment section.

Evaluating the Order Parameters from the ESR Spectra

The coefficients $g^{\ell}_{m,n}(H)$ are functions of the static magnetic field strength. The ESR spectrum is built up from a linear combination of these coefficients as shown by Eq. 4. In our method the $g^{\ell}_{m,n}(H)$'s are thought of as a basis set that spans the space occupied by ESR spectra. Our task is to measure the amount of each basis spectra, i.e., the value of $a^{\ell}_{m,n}$, contained in an ESR spectrum.

Let the indices i, j, and k represent the triplets of indices (ℓ, m, n), (ℓ', m', n'), and (ℓ'', m'', n''). We define a projection operator q_i by the equation

$$q_i(H) = \sum_j \alpha_{i,j}\, g_j(H), \tag{13}$$

where $\alpha_{i,j}$ is a matrix element independent of H, and g_j are the basis spectra $g^{\ell}_{m,n}(H)$. We require that $q_i(H)$ have the property,

$$\langle q_i g_k \rangle \equiv \int_0^{\infty} dH\, q_i^*(H)\, g_k(H) = \delta_{i,k}. \tag{14}$$

The projection operator q_i is used to measure the contribution to the ESR spectrum $F(H)$, from the ith basis spectrum g_i, given by moment a_i, since by Eqs. 14 and 4,

$$a_i = \langle q_i F \rangle. \tag{15}$$

We construct the operator q_i using coefficients $\alpha_{i,j}$ where the $\alpha_{i,j}$'s are found from substituting Eq. 13 into Eq. 14 and solving for $\alpha_{i,j}$. We find

$$\alpha_{i,j} = \langle g_i g_j \rangle^{-1}, \tag{16}$$

where $\langle g_i g_j \rangle^{-1}$ is the i, jth element of the inverse of the matrix with elements $\langle g_i g_j \rangle$.

From the expression for $g_i(H)$ from Eqs. 5b and 7, and for the Lorentzian line shape of Eq. 6, it can be shown that

$$\langle g_i g_j \rangle = \sqrt{\frac{2\ell + 1}{8\pi^2}} \sqrt{\frac{2\ell' + 1}{8\pi^2}} \int_{C_0} \int_{C_0} d\Omega d\Omega'\, D^{*\ell}_{m,n}(\Omega)\, D^{\ell'}_{m',n'}(\Omega') \times \sum_{I,J} \frac{2\epsilon}{4\epsilon^2 + [H^I_0(\Omega) - H^J_0(\Omega')]^2}. \tag{17}$$

The elements $\langle g_i g_j \rangle^{-1}$ can thus be calculated by inversion of the matrix $\langle g_i g_j \rangle$, calculated by numerical integration of Eq. 17.

When the $g^{\ell}_{m,n}$'s are not independent we must take care in computing the inverse to the matrix in Eq. 17, since if g_i and g_j are equal to within a multiplicative constant (i.e., their shapes overlap) then the matrix is singular and its inverse does not exist. Even when they are only approximately equal, matrix inversion may be difficult. This problem would lead to difficulty in distinguishing order parameters that correspond to overlapping basis spectra.

The line shape parameters, h_n, are determined in a

manner analogous to the determination of the order parameters. We define the basis spectra $\Gamma_n(H)$ for a random, immobile ESR spectrum such that

$$\Gamma_n(H) = \frac{1}{12\pi^2\epsilon}\int_{C_0} d\Omega\, P_n[y_l(H,\Omega)], \tag{18}$$

where y_l is defined in Eq. 12. The observed signal $F_{\text{random}}(H)$ is then

$$F_{\text{random}}(H) = \frac{1}{8\pi^2}\int_{C_0} d\Omega\, G^*(H,\Omega) = \sum_{n=0}^{\infty} h_n \Gamma_n(H). \tag{19}$$

Replacing $g_i(H)$ with $\Gamma_i(H)$ in Eqs. 13 and 14 to calculate the new projection operators r_i we find

$$h_n = \langle r_n F_{\text{random}} \rangle. \tag{20}$$

Symmetry Properties

The laboratory frame z axis is chosen in the direction of the static magnetic field so that $\mathbf{K}_{\text{lab}} = (0, 0, 1)$. From Eq. 9, $\mathbf{K}(\Omega)$ is then

$$\begin{aligned} K_{[x,y]} &= \sin\beta[\sin(\gamma+\alpha_0)\{\sin\gamma_0, \cos\gamma_0\} \\ &\quad + \cos(\gamma+\alpha_0)\cos\beta_0\{-\cos\gamma_0, \sin\gamma_0\}] \\ &\quad - \sin\beta_0\cos\beta\{\cos\gamma_0, \sin\gamma_0\} \\ K_z &= \cos\beta\cos\beta_0 - \sin\beta\sin\beta_0\cos(\gamma+\alpha_0). \end{aligned} \tag{21}$$

$\mathbf{K}(\Omega)$ in Eq. 21 is independent of Euler angle α, so that, from Eqs. 6 and 7 or eqs. 11 and 7, $G(H, \Omega)$ is also independent of α. Using Eqs. 3 and 5b it can then be shown that $g^{\ell}_{m,n} = \delta_{m,0} g^{\ell}_{0,n}$ so that the ESR spectrum contains no information about the angular distribution of spin probes about the laboratory frame z axis.[1]

The Wigner matrix elements are related to the spherical harmonics $Y_{\ell,n}(\beta, \gamma)$ by (Davydov, 1966)

$$D^{\ell}_{0,n}(\Omega) = \left(\frac{4\pi}{2\ell+1}\right)^{1/2} Y_{\ell,n}(\beta,\gamma) \tag{22}$$

so that

$$g^{\ell}_{0,n}(H) = \sqrt{2\pi}\int_0^{2\pi} d\gamma \int_0^{\pi} d\beta \sin\beta\, G(H,\beta,\gamma)\, Y^*_{\ell,n}(\beta,\gamma). \tag{23}$$

With Eq. 23 we can derive a restriction on the index ℓ. Under the inversion of coordinates $\beta \rightarrow \pi - \beta$ and $\gamma \rightarrow \gamma + \pi$, it holds that $Y_{\ell,n}(\pi-\beta, \gamma+\pi) = (-1)^{\ell} Y_{\ell,n}(\beta,\gamma)$, while $G(H, \beta, \gamma)$ is invariant. This implies, using Eq. 23, that $g^{\ell}_{0,n} = 0$ unless ℓ is an even integer. The restriction on ℓ indicates that when $H^1_0(\Omega)$ is given by Eq. 7 and $G(H, \beta, \gamma)$ is given by Eqs. 6 or 11 the ESR technique detects only moments of the angular distribution $N(\Omega)$ that have even ℓ.

The orientation of the spin probe relative to the elemental frame, described by Ω_0, is generally not known. When $\Omega_0 = 0$, $N(\Omega)$ describes the angular arrangement of the spin probes themselves and not the elements to which they are attached. Substituting $\alpha_0 = \beta_0 = \gamma_0 = 0$ into Eq. 21, we find $\mathbf{K} = (-\sin\beta\cos\gamma, \sin\beta\sin\gamma, \cos\beta)$ and we can derive a restriction on index n of $g^{\ell}_{0,n}$ in Eq. 23. Under inversion of the z axis $\beta \rightarrow \pi - \beta$ and $Y_{\ell,n}(\pi-\beta, \gamma) = (-1)^{\ell+n} \cdot Y_{\ell,n}(\beta,\gamma)$ while $G(H, \beta, \gamma)$ is invariant. This property requires $g^{\ell}_{0,n} = 0$ unless n is an even integer. All of the restrictions on ℓ, m, and n require $g^{\ell}_{m,n} = 0$ unless $m = 0$ and ℓ, $n = 0, 2, 4, \ldots$. These same restrictions apply for the derivative basis spectra generated using Eqs. 5b and 8.

It is important in our application to the muscle fibers to notice that Eqs. 21 and 23 imply that for no choice of Ω_0 can the ESR spectrum depend on moments $a^{\ell}_{0,n}$ where $n \neq 0$ unless elemental angular distribution also depends on γ. This means that if the ESR spectrum of a muscle fiber contains basis spectra $g^{\ell}_{0,n}$ when $n \neq 0$, then the elemental (cross-bridge) angular distribution depends on γ.

Application to Muscle Fibers

The orientational order of myosin cross-bridges in muscle fibers has been investigated using ESR (Thomas and Cooke, 1980; Cooke et al., 1982). In these experiments the S-1 moiety of the cross-bridge is specifically labeled at a single SH group with a nitroxide spin probe. A small bundle of 20–50 aligned fibers is used in an experiment. Because of the number of fibers, the bundle is cylindrically symmetrical about the fiber axis. Symmetry about the fiber axis is also observed in single fibers by fluorescence polarization (Burghardt et al., 1983). Thus, no information is lost by aligning the fiber axis along the magnetic field.

Fig. 1 shows a typical ESR spectrum for spin-labeled S-1 of myosin that has been precipitated with ammonium sulfate (a generous gift from David Thomas of the University of Minnesota, Minneapolis, MN). The spin probes are in an environment very similar to that of spin-labeled muscle fibers, but the probes are randomly oriented and effectively immobile. The spectrum has been fit to a function of the form of Eq. 1 with $N(\Omega) = 1/(8\pi^2)$ and $G^*(H, \Omega)$ obtained from both the Lorentzian line shape of Eq. 8 and from the generalized line shape of Eq. 11. The best fit of this spectrum for the Lorentzian line shape is $g_x = 2.0084$, $g_y = 2.0063$, $g_z = 2.0026$, $T_x = 7.92$, $T_y = 7.78$, $T_z = 34.8$, and $\epsilon = 2.42$. The best fit for the generalized line shape is $g_x = 2.0083$, $g_y = 2.0062$, $g_z = 2.0025$, $T_x = 7.7$, $T_y = 7.6$, $T_z = 34.9$, and $\epsilon = 4.9$. The values for h_n for this fit are shown in Table I.

Both line shapes and their parameter values are used to calculate $g^{\ell}_{0,n}$ from Eq. 5b. We have used $\ell \leq 8$ in the analysis with the restriction that ℓ and n are even. From the values of $g^{\ell}_{0,n}(H)$ and Eqs. 13, 16, and 17, the projection

[1] Information on order about this z axis can be obtained by reorienting the assembly in the static magnetic field and redefining the Euler angles relative to a new lab frame.

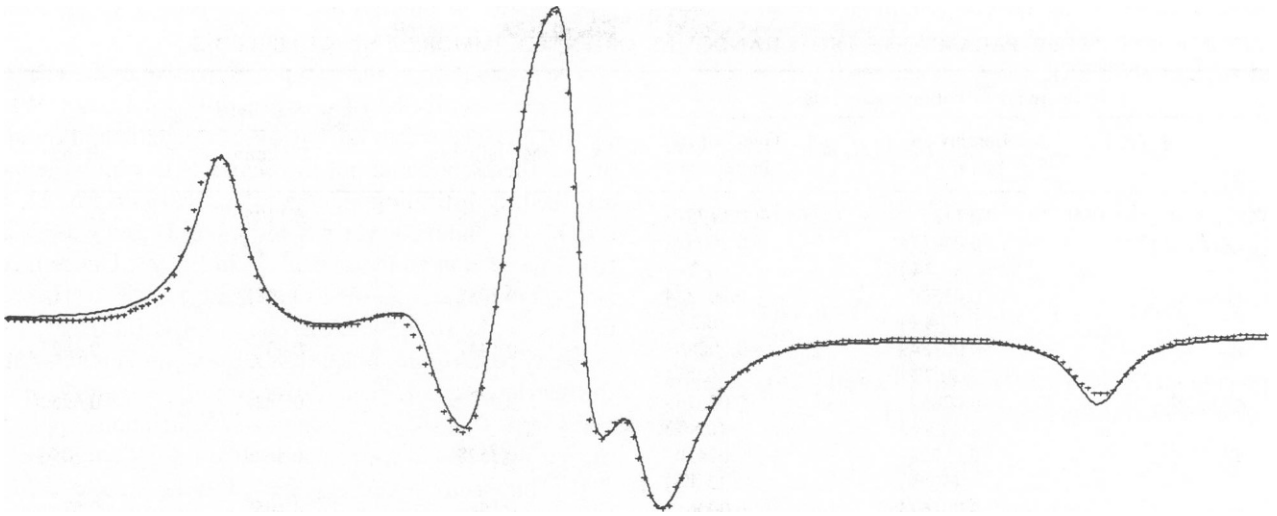

FIGURE 1 The ESR spectrum from randomly oriented, immobilized, spin-labeled S-1 of myosin. The theoretical fit (solid line) is generated from a random distribution with a Lorentzian line shape (see Eq. 6) such that $g_x = 2.0084$, $g_y = 2.0063$, $g_z = 2.0026$, $T_x = 7.92$, $T_y = 7.78$, $T_z = 34.8$, and $\epsilon = 2.42$. Varying along the abscissa is the magnitude of the static magnetic field; it ranges over 100 G.

operators $q_i(H)$ are calculated. The coefficients $a^{\ell}_{0,n}$ can then be measured from any spectrum using the projection operators and Eq. 15.

When we generate a theoretical random spectrum using $G(H, \Omega)$ with the above parameter values and $N(\Omega) = 1/(8\pi^2)$ in Eq. 1, and then solve for $a^{\ell}_{m,n}$ using the projection operators and Eq. 15, we find $a^0_{0,0} = 1/\sqrt{8\pi^2}$ and all other coefficients for $\ell < 8$ are $\leq 10^{-6}$ for either line shape. This indicates that enough terms of the matrix in Eq. 17 were included so that the inverse matrix in Eq. 16 was accurately determined. When the random experimental spectrum is used with the projection operators and Eq. 15, we find $a^0_{0,0} = 1/\sqrt{8\pi^2}$ for both line shapes. However, for both line shapes a few of the higher order parameters corresponding to nonrandom distributions are not negligibly small. The values of these order parameters are listed in Table II.

TABLE I
GENERALIZED LINE SHAPE EXPANSION PARAMETERS

n	h_n	n	h_n
0	1.000	6	0.7992
1	−0.1944	7	0.6040
2	−1.0540	8	0.1455
3	−0.9880	9	−0.0518
4	−0.7049	10	−0.1282
5	0.0055	11	−0.2103

Legendre polynomial expansion coefficients h_n for the generalized line shape treatment of randomly oriented, immobilized spin-labeled S-1. The ESR spectrum of randomly oriented immobilized spin probes, covalently and specifically attached to S-1 of myosin, as shown in Fig. 1, was fit to the Legendre polynomial expansion of Eq. 11. Shown are the values of h_n for this generalized line shape normalized so that $h_0 = 1$.

The order parameters $a^6_{0,6}$ and $a^8_{0,6}$ are not negligibly small for the random spectrum because their corresponding basis spectra overlap significantly with the random basis spectra. The basis spectra would overlap less if the $\underline{g}$ and $\underline{T}$ tensor values were more anisotropic, causing the ESR spectrum to become more sensitive to γ dependence in the probe angular distribution. We also found that increasing the number of coefficients in the sum to $\ell \geq 10$ does not decrease the values of $a^{\ell}_{m,n}$ for $\ell > 0$ in Table II. Also, the values of $a^{\ell}_{m,n}$ for $\ell > 0$ obtained from independently obtained random spectra do not average to zero. Because the Lorentzian line shape treatment is so close an approximation to the real line shape as shown by Table II, we choose to use the Lorentzian line shape in the analysis of spectra from muscle fibers (see below).

Fig. 2 shows an experimental ESR spectrum (a generous gift from David Thomas at the University of Minnesota, Minneapolis, MN) for maleimide spin-labeled muscle fibers in rigor. The rigor state of muscle occurs in the absence of ATP and has been shown to be a highly ordered, static state, where nearly all of the cross-bridges are attached to adjacent actin filaments (Cooke and Franks, 1980; Thomas et al., 1980). The fiber axis was aligned with the applied magnetic field.

In the ideal case, the $q_i(H)$ calculated above from the randomly oriented spectrum would be applied to the spectrum $F(H)$ obtained from rigor fibers to determine the distribution coefficients using Eq. 15. However, we find that the theoretical spectrum generated using these so-determined distribution coefficients in Eqs. 1 and 2 does not best fit the experimental spectrum (according to a chi-squared analysis) if we allow the $\underline{g}$ and $\underline{T}$ tensor values to vary freely. The best fit values are different from the values derived from the random spectrum. (This could be

TABLE II
ORDER PARAMETERS FROM RANDOMLY ORIENTED, IMMOBILE SPIN-LABELED S-1

	Measured distribution coefficients		Theoretical limits		
	Lorentzian line shape	Generalized line shape	Minimum	Maximum	Range
$a^0_{0,0}$	0.1125	0.1125	0.1125	0.1125	0
$a^2_{0,0}$	0.004474 (1.2%)	−0.000597 (0.2%)	−0.1258	0.2516	0.3774
$a^2_{0,2} + a^2_{0,-2}$	−0.01500 (2.4%)	−0.001384 (0.2%)	−0.3082	0.3082	0.6164
$a^4_{0,0}$	−0.003549 (0.7%)	−0.000867 (0.2%)	−0.1447	0.3376	0.4823
$a^4_{0,2} + a^4_{0,-2}$	−0.02652 (3.9%)	−0.005769 (0.8%)	−0.3432	0.3432	0.6864
$a^4_{0,4} + a^4_{0,-4}$	−0.05222 (7.4%)	0.02410 (3.4%)	−0.3528	0.3528	0.7056
$a^6_{0,0}$	0.001674 (0.3%)	0.000619 (0.1%)	−0.1683	0.4058	0.5741
$a^6_{0,2} + a^6_{0,-2}$	−0.001989 (0.2%)	−0.009198 (1.1%)	−0.4026	0.4026	0.8052
$a^6_{0,4} + a^6_{0,-4}$	−0.02039 (1.6%)	0.03802 (2.9%)	−0.6470	0.6470	1.2940
$a^6_{0,6} + a^6_{0,-6}$	0.1121 (14.5%)	0.07603 (9.9%)	−0.3854	0.3854	0.7708
$a^8_{0,0}$	−0.000335 (.05%)	−0.004416 (0.7%)	−0.1901	0.4676	0.6577
$a^8_{0,2} + a^8_{0,-2}$	−0.007798 (0.9%)	−0.005076 (0.6%)	−0.4581	0.4581	0.9162
$a^8_{0,4} + a^8_{0,-4}$	0.02701 (3.6%)	0.01890 (2.5%)	−0.3792	0.3792	0.7584
$a^8_{0,6} + a^8_{0,-6}$	0.07831 (10.9%)	0.09450 (13.1%)	−0.3606	0.3606	0.7212
$a^8_{0,8} + a^8_{0,-8}$	−0.001390 (0.2%)	0.09062 (11.0%)	−0.4113	0.4113	0.8226

The spectrum shown in Fig. 2 was analyzed as a general, nonrandom distribution of probes, for both Lorentzian and generalized line shapes. Shown are the values of the order parameters obtained in these analyses. Shown also are the theoretical maximum and minimum values for each parameter (e.g., Thompson et al., 1984). The value under each order parameter is the percentage of the range each order parameter makes.

due to environmental changes). A more appropriate random spectrum might be measured from spin-labeled cross-bridges in myofibrils.

Fig. 2 shows the theoretical spectra obtained from the linear combination of basis spectra using Eq. 4 and the Lorentzian line shape. The best fit values for the experimental parameters are $g_x = 2.0082$, $g_y = 2.0042$, $g_z = 2.0019$, $T_x = 7.5$, $T_y = 7.0$, $T_z = 31.4$, and $\epsilon = 2.8$. The values of the order parameters are shown in Table III.

The estimation of random error in the order parameters due to noise in the spectra or from nonuniformity in the biological sample would be carried out by fitting several spectra from different samples, under identical conditions. The measured order parameters are then averaged.

Of the 25 moments that correspond to the contributions from the $\ell \leq 8$ basis spectra (with the restriction that ℓ and n are even integers), one is determined from the normalization of the angular distribution. We choose the normalization

$$\int_0^{2\pi} d\alpha \int_0^{\pi} \sin\beta d\beta \int_0^{2\pi} d\gamma\, N(\Omega) = 1 \qquad (24)$$

so that $N(\Omega) \sin\beta\, d\beta d\gamma\, d\alpha$ is the probability that a probe is oriented between α, β, γ and $\alpha + d\alpha$, $\beta + d\beta$, $\gamma + d\gamma$. This implies that $a^0_{0,0} = 1/\sqrt{8\pi^2}$. Of the remaining 24, only 14 independent quantities can be measured from the ESR spectrum because, as can be shown from Eq. 23, the technique cannot distinguish moments $a^\ell_{0,n}$ from $a^\ell_{0,-n}$ for $n > 0$. The measured quantity is the sum $a^\ell_{0,n} + a^\ell_{0,-n}$.

From Table III we see that moments corresponding to γ dependence in the angular distribution are not all zero (moments $a^\ell_{0,n}$ with $n \neq 0$). Angle γ is related to the torsional degree of freedom of the myosin cross-bridge (Wilson and Mendelson, 1983; Mendelson and Wilson, 1982; Morales, 1984). As we stated before, γ dependence in the spin probe distribution also implies γ dependence in the cross-bridge angular distribution. This indicates the cross-bridge binds to actin at fixed torsional angles as has been assumed previously (Thomas and Cooke, 1980; Mendelson and Wilson, 1982).

There has been speculation (Mendelson and Wilson, 1982) that the S-1 moiety may have complete torsional freedom when unattached to actin. The unattached (or

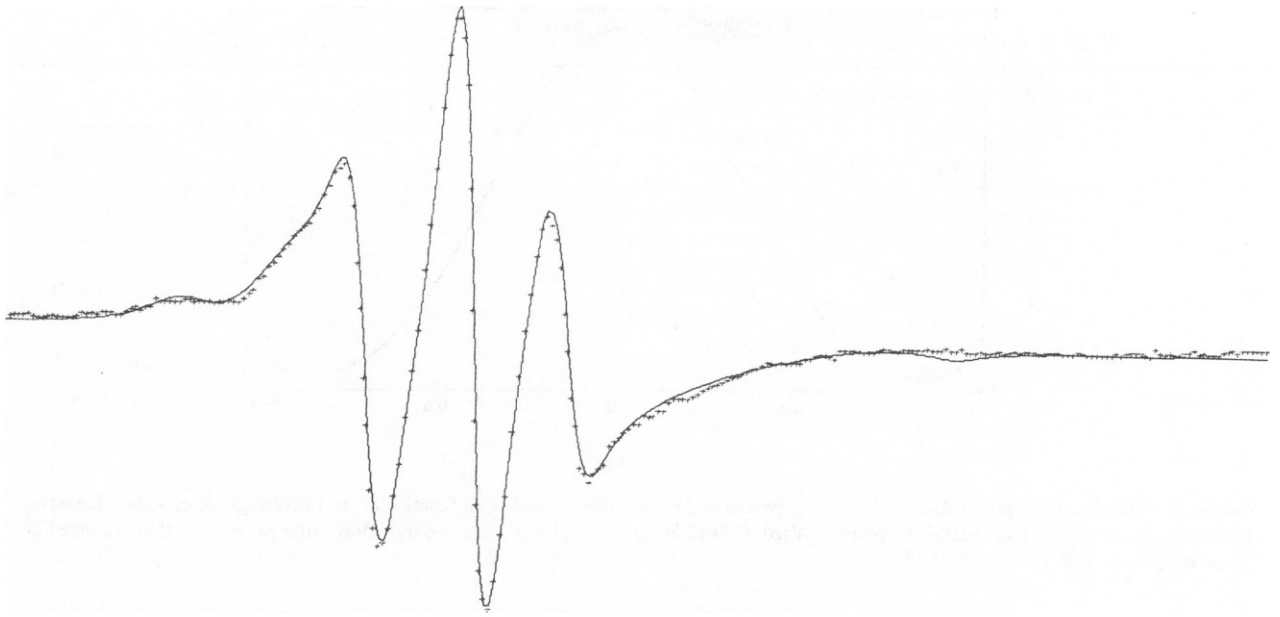

FIGURE 2 The ESR spectrum of a spin labeled muscle fiber in rigor (i.e., in the absence of ATP) and the best theoretical fit (solid line) found using the model independent analysis such that $g_x = 2.0082$, $g_y = 2.0042$, $g_z = 2.0019$, $T_x = 7.5$, $T_y = 7.0$, $T_z = 31.4$, and $\epsilon = 2.8$. Varying along the abscissa is the magnitude of the static magnetic field; it ranges over 100 G.

relaxed) state is induced in a muscle fiber by adding ATP to the rigor solution. Future application of model-independent ESR will likely resolve this question.

The probe distribution in β (the angle from the fiber axis) is given by

$$\mathcal{N}(\beta) = \int_0^{2\pi} d\alpha \int_0^{2\pi} d\gamma\, N(\Omega) = 2\pi \sum_{\ell=0}^{\infty} a^{\ell}_{0,0} \left(\frac{2\ell+1}{2}\right)^{1/2} P_{\ell}(\cos\beta), \quad (25)$$

TABLE III
ORDER PARAMETERS FOR RIGOR FIBERS

$a^0_{0,0}$	0.1125	$a^6_{0,4} + a^6_{0,-4}$	0.292 (22.6%)
$a^2_{0,0}$	−0.0807 (21.4%)	$a^6_{0,6} + a^6_{0,-6}$	0.312 (40.5%)
$a^2_{0,2} + a^2_{0,-2}$	−0.0396 (6.4%)	$a^8_{0,0}$	0.00312 (0.5%)
$a^4_{0,0}$	0.0425 (8.8%)	$a^8_{0,2} + a^8_{0,-2}$	−0.0110 (1.2%)
$a^4_{0,2} + a^4_{0,-2}$	−0.0174 (2.5%)	$a^8_{0,4} + a^8_{0,-4}$	−0.0297 (3.9%)
$a^4_{0,4} + a^4_{0,-4}$	−0.239 (33.9%)	$a^8_{0,6} + a^8_{0,-6}$	0.188 (26.1%)
$a^6_{0,0}$	−0.0113 (2.0%)	$a^8_{0,8} + a^8_{0,-8}$	0.563 (68.4%)
$a^6_{0,2} + a^6_{0,-2}$	−0.0236 (2.9%)		

The order parameters from spin labeled cross-bridges in muscle fibers in rigor. The ESR spectrum of Fig. 3 was used in the analysis. The values of the moments are used to calculate the angular distributions plotted in Figs. 3 and 4. The value under each order parameter is the percentage of the range each order parameter makes.

where P_{ℓ} is a Legendre polynomial. It is likely that the distribution of cross-bridges is symmetric about $\beta = 90°$ (Morales, 1984). In this case, the coefficients $a^{\ell}_{0,0}$ with odd ℓ are zero and the even terms in the sum, which can be calculated using coefficients obtained from the ESR spectra, adequately describe $\mathcal{N}(\beta)$.

Fig. 3 shows $\mathcal{N}(\beta)$ measured from the ESR spectrum of Fig. 2 of a muscle fiber in rigor. In Fig. 3 we have plotted $\mathcal{N}(\beta)$ as a function of $x = \cos\beta$. As shown, the distribution peaks at $\beta = 90°$. This does not indicate that the distribution in a single sarcomere peaks at $\beta = 90°$; the sum of two distributions about the angles $90° - \eta$ and $90° + \eta$ can also peak at 90°.

Fig. 4 shows $N(\Omega)$ measured from the ESR spectrum of Fig. 3 and plotted as a function of γ when $\beta = 90°$. Because of the symmetry requirement that $a^{\ell}_{0,n} = 0$ unless n is an even integer, the measured distribution in Fig. 4 must be even about $\gamma = \pi$. As shown, the distribution contains maxima near $\gamma = 45°$, 135°, 225°, and 315° indicating the probes have preferred γ orientations. The plot also shows that there are probably two preferred probe orientations in γ indicating possibly two preferred cross-bridge orientations. This would be consistent with rigor cross-bridges attaching to actin with equal probability at one of two binding sites at different γ angles.

The resolution of the γ dependence from the ESR spectrum is less than that of the β dependence as evidenced by the negative values of N, for some γ, as shown in Fig. 4. It should be possible to increase resolution in γ by increasing the number of the fitting parameters.

Truncation of the theoretical fit at $\ell \leq 8$ introduces error in the projection operator q_i since the correct projection

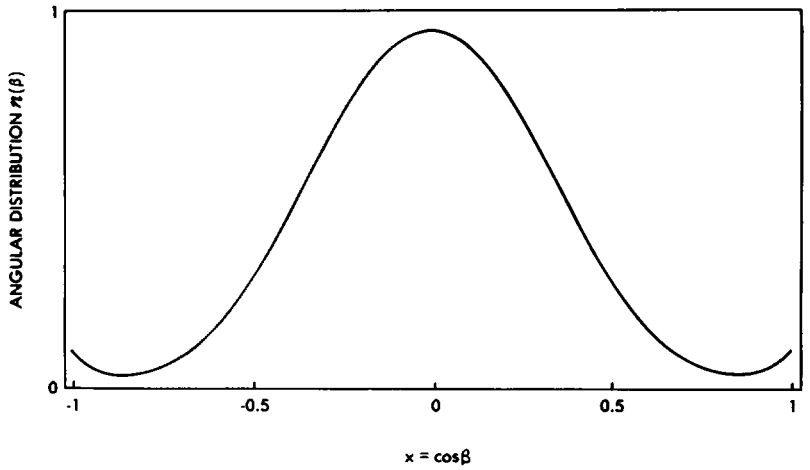

FIGURE 3 The observed angular distribution of spin probes in a muscle fiber in rigor as a function of the Euler angle β, measured from the ESR spectrum in Fig. 2. The angular distribution $\mathcal{N}(\beta)$, defined in Eq. 25, is plotted vs. $x = \cos\beta$. Only order parameters that are listed in Table III are included.

operator is made up of all orders of basis spectra.[2] Higher order ($\ell \geq 10$) basis spectra do contribute to the spectrum but all of the obvious features of the spectrum are present in our approximate fit.

CONCLUSION

Measurement of the angular distribution function of ordered probes has been the object of many experiments employing fluorescence polarization (Burghardt et al., 1983; Wilson and Mendelson, 1982; Borejdo et al., 1982; Thompson et al., 1984) and ESR (Thomas and Cooke, 1980; Cooke et al., 1982). In the past, data analysis from these techniques was model dependent in that data was fit to a plausible guess for the functional form of the orientation distribution. Here, as in previous related papers (Burghardt, 1984; Burghardt et al. 1983; Thompson et al., 1984; Hentschel et al., 1978; Friesner et al., 1979), an approach to this problem in which a model is not required has been presented. As in the previous analysis with fluorescence polarization, the model-independent approach to ESR has several advantages over model-dependent descriptions, such as defining the theoretical limitations on the sensitivity of the ESR technique and relating observable quantities to the symmetry properties of the assembly. The model-independent approach is a good starting point for data analysis before a model is chosen since the order parameters can be related to the free parameters from any model. By this feature the validity of many models can be easily tested. Most importantly this method removes the bias accompanying a chosen model and allows experimental results to be reported in an unambiguous way.

[2]When the line width ϵ approaches zero, matrix element $\langle g_i g_j \rangle$ approaches $\delta_{i,j}$ (see Eq. 17), which is a special case in which q_i consists of a single term. Thus, in practice, only when the line width ϵ approaches zero can the ESR spectrum be unambiguously interpreted in its description of elemental order.

The authors thank David Thomas, Roger Cooke, Mark Crowder, and Anthony Baker for generous gifts of ESR data; Manuel F. Morales for helpful discussions; and Joan Junkin for help in typing the manuscript.

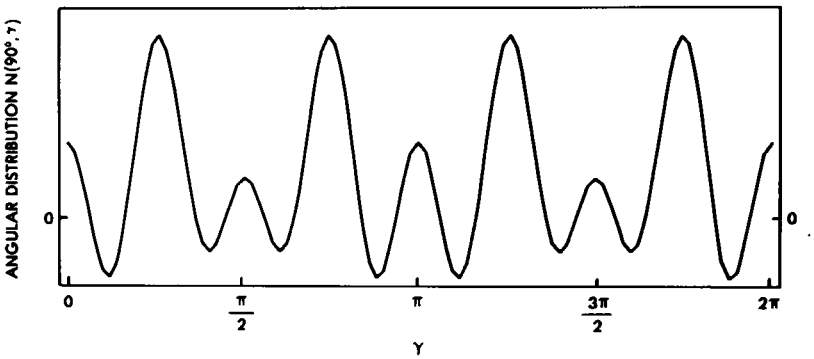

FIGURE 4 The observed angular distribution of spin probes in a muscle fiber in rigor as a function of Euler angle γ at $\beta = 90°$, measured from the ESR spectrum in Fig. 2. Only order parameters that are listed in Table III are included.

This work was supported by American Heart Association Postdoctoral Fellowship 82 071 (to T. P. Burghardt), Damon Runyon-Walter Winchell Cancer Fund Postdoctoral Fellowship 593 (to N. L. Thompson), and by grants (to Manuel F. Morales) HL-16683 from U.S. Public Health Service and PCM-7922174 from the National Science Foundation.

Received for publication 22 February 1984 and in final form 25 April 1985.

REFERENCES

Arfken, G. 1970. Special functions. *In* Mathematical Methods for Physicists. Academic Press, Inc., New York. 609–616.

Berliner, L. J., editor. 1976. Spin Labeling: Theory and Applications. Academic Press, Inc., New York. 1–592.

Borejdo, J., O. Assulin, T. Ando, and S. Putnam. 1982. Cross-bridge orientation in skeletal muscle measured by linear dichroism of an extrinsic chromophore. *J. Mol. Biol.* 158:391–414.

Burghardt, T. P. 1984. Model-independent fluorescence polarization for measuring order in a biological assembly. *Biopolymers.* 23:2383–2406.

Burghardt, T. P., T. Ando, and J. Borejdo. 1983. Evidence for cross-bridge order in contraction of glycerinated skeletal muscle. *Proc. Natl. Acad. Sci. USA.* 80:7515–7519.

Cooke, R., M. Crowder, and D. D. Thomas. 1982. Orientation of spin labels attached to cross-bridges in contracting muscle fibers. *Nature (Lond.).* 300:776–778.

Cooke, R., and K. Franks. 1980. All myosin heads form bonds with actin in rigor rabbit skeletal muscle. *Biochemistry.* 19:2265–2269.

Davydov, A. S. 1966. Quantum Mechanics. N.E.O. Press, Ann Arbor, Michigan. 153–170.

Friesner, R., J. A. Nairn, and K. Sauer. 1979. Direct calculation of the orientational distribution of partially ordered ensembles from the EPR line shape. *J. Chem. Phys.* 71:358–365.

Goldman, S. A., G. V. Bruno, C. F. Polnaszek, and J. F. Freed. 1972. An ESR study of anisotropic rotational reorientation and slow tumbling in liquid and frozen media. *J. Chem. Phys.* 56:716–735.

Goldstein, H. 1980. Classical Mechanics. Addison-Wesley, Reading, MA. 107–109.

Hentschel, R., J. Schlitter, H. Sillescu, and H. W. Speiss. 1978. Orientational distributions in partially ordered solids as determined from NMR and ESR line shapes. *J. Chem. Phys.* 68:56–66.

Hudson, A., and G. R. Luckhurst. 1968. The electron resonance line shapes of radicals in solution. *Chem. Rev.* 69:191–225.

Libertini, L. J., C. A. Burke, P. C. Jost, and O. H. Griffith. 1974. An orientation distribution model for interpreting ESR line shapes of ordered spin label. *J. Magn. Res.* 15:460–476.

McCalley, R. C., E. J. Shimshick, and H. M. McConnell. 1972. The effect of slow rotational motion on paramagnetic resonance spectra. *Chem. Phys. Lett.* 13:115–119.

Mendelson, R. A., and M. Wilson. 1982. Three-dimensional disorder of dipolar probes in a helical array. *Biophys. J.* 39:221–227.

Morales, M. F. 1984. Calculation of the polarized fluorescence from a labeled muscle fiber. *Proc. Natl. Acad. Sci. USA.* 81:145–149.

Polnaszek, C. F., and J. H. Freed. 1975. Electron spin resonance studies of anisotropic ordering, spin relaxation, and slow tumbling in liquid crystalline solvents. *J. Phys. Chem.* 79:2283–2308.

Thomas, D. D., and R. Cooke. 1980. Orientation of spin-labeled myosin heads in glycerinated muscle fibers. *Biophys. J.* 32:891–906.

Thomas, D. D., S. Ishiwata, J. C. Seidel, and J. Gergely. 1980. Submillisecond rotation dynamics of spin-labeled myosin heads in myofibrils. *Biophys. J.* 32:873–889.

Thompson, N. L., H. M. McConnell, and T. P. Burghardt. 1984. Order in supported phospholipid monolayers detected by the dichroism of fluorescence excited with polarized evanescent illumination. *Biophys. J.* 46:739–747.

Wilson, M., and R. A. Mendelson. 1983. A comparison of order and orientation of cross-bridges in rigor and relaxed muscle fibers using fluorescence polarization. *J. Muscle Res. Cell Motil.* 4:671–693.